

## THE INFLUENCE OF MORTAR AIR CONTENT AND FLUIDITY ON SURFACE VOID CHARACTERISTICS IN SELF-COMPACTING CONCRETE

(Translation from Proceedings of JSCE, No. 711 /V-56, August 2002)



Kazuo ICHIMIYA



Takashi IDEMITSU



Takehiro YAMASAKI

With the aim of reducing surface voids in powder-type self-compacting concrete, this paper presents a discussion of the effects of air content and fluidity, as well as the various types of form-release agent. Two combinations of superplasticizer (SP) and air-adjusting agent are used in this research. One is a naphthalene-based SP with an added air-entraining agent, and the other is a polycarboxylic acid SP with an added defoaming agent. The settling behavior of coarse aggregate and the rising of air voids are explained in terms of the equilibrium among the forces of buoyancy, gravity, and fluid resistance. Coarse aggregate particles and internal voids are assumed to be spherical solid bodies. The fluid resistance of mortar is expressed in terms of rheological constants (yield value and plastic viscosity). Using this equilibrium-based approach, and taking account of adhesion to the form, it is shown that the separation of surface voids from the form can be explained.

**Keywords:** *self-compacting concrete, surface void, concrete product, air content, rheological constants*

---

Kazuo Ichimiya is an associate professor in the Department of Civil Engineering at Oita National College of Technology, Japan. He obtained his D. Eng. from the Kyushu Institute of Technology in 2002. His research interest includes self-compacting concrete. He is a member of JSCE and JCI.

---

Takashi Idemitsu is a professor in the Department of Civil Engineering at Kyushu Institute of Technology, Japan. He obtained his D. Eng. from the Kyushu Institute of Technology in 1992. His research interest includes improvement of construction technique of prestressed concrete and self-compacting concrete. He is a member of JSCE and JCI.

---

Takehiro Yamasaki is a professor in the Department of Civil Engineering at Kyushu Institute of Technology, Japan. He obtained his D. Eng. from the Kyoto University in 1989. His research interest includes polymer-cement concrete, performance of chemical admixtures, and self-compacting concrete. He is a member of JSCE and JCI.

---

## **1. INTRODUCTION**

The use of self-compacting concrete eliminates much of the noise and vibration caused by concrete placing, while also achieving labor-saving in construction work. The concrete can be easily placed anywhere within form containing complex reinforcement arrangements without the need for compaction[1][2]. However, air entrapped in the concrete during mixing and placing appears in the form of voids at the surface as a result of the concrete's high viscosity. These "surface voids" cause certain problems, such as reduced commercial value resulting from the degraded appearance. Further, in a freeze-thaw environment, surface voids contribute to deterioration and durability is reduced[3].

Surface void generation is affected by (a) the concrete itself, (b) the chemical admixtures used, (c) the form-release agent, and (d) the placing method. Each involves several possible factors, such as (a) the materials used, the mix proportion, and the physical properties of the concrete (slump flow and air content), (b) the surface tension of the chemical admixture, the form-release agent, the amount of defoaming agent used, (c) the type of form-release agent and surface-active agent, and (d) the form shape and material, the height and rate of placement, and the use of low-frequency vibration for compaction[4].

In this research, concrete air content and fluidity are chosen from among these factors for a focused study of the relation between them and the generation of surface voids. The relationship between air content and surface voids is examined by measuring the size and quantity of surface voids, which are influenced by the type and air entraining action of superplasticizer (SP).

Slump flow, a measure of concrete fluidity, heavily influences the generation of surface voids; the greater the slump flow, the lower the density of surface voids becomes[5][6][7]. However, the migration characteristics of voids in concrete cannot be explained theoretically because slump flow depends on other technical parameters. Therefore, in this work, concrete fluidity is expressed in terms of the rheological constants yield value ( $\tau$ ) and plastic viscosity ( $\eta_p$ )[8].

Before attempting to explain the migration of surface voids, the migration characteristics of coarse aggregate particles and internal voids are explained in terms of the equilibrium of forces acting on each particle. These forces include gravity, buoyancy, and fluid resistance all rheological constants of the mortar. Next, in order to explain the theoretical relationship between mortar fluidity and the maximum surface void diameter, the migration of surface voids is explained in terms of the equilibrium among gravity, buoyancy, fluid resistance, and adhesion to the form.

Concrete surface tension is expressed throughout in terms of the surface tension of the paste, because aggregate is known to not have an influence. Moreover, in the theoretical consideration, the inclination of the form was assumed to be zero degrees (upper surface of form horizontally set up), while experiments were carried out with a form inclined at 90 degrees (form vertically set up). In past research, the authors have found that the size and quantity of surface voids generated is almost the same for inclination angles from 0 to 110 degrees[9].

## **2. BASIC THEORY**

### **(1) Influence of type and air-entraining action of SP on surface void characteristics**

When a polycarboxylic acid SP is used, a defoaming agent is also added to the mix to compensate for the increased air content, because the SP has an air-entraining ability[10]. However, the defoaming mechanism is unclear, and there is no standard method of evaluating the performance of defoaming agents. In general, the defoaming agent does not influence the overall characteristics of the concrete (fluidity, strength, and deformation), because it is a trace component (0.0001-0.1% of the cement mass). However, there has until now been no investigation of the influence of defoaming agents on surface voids[11].

Moreover, naphthalene-based SP, which have no air-entraining ability, are also used in concrete production. These are advantageous because air voids expand with the heat of steam curing, yet lower air content is desired in concrete production. However, if the air content is increased to 3-6% using an air-entraining admixture, resistance to freeze-thaw action must be improved.

Thus, the surface void characteristics will be influenced by the type of SP, the type of air-entraining admixture, and their combination.

(2) Influence of paste surface tension on diameter of internal and surface voids

The internal forces acting on a void in self-compacting concrete are illustrated in **Figure 1**. The differential pressure between outside and inside of an internal void (internal pressure difference), the paste surface tension, and the diameter of internal voids are expressed by the symbols  $\Delta p$ ,  $\gamma_L$ , and  $d_v$  respectively. Here,  $d_v$  can be calculated using **Expression (1)**, which is a transformation of the balance between the resultant of internal pressure differential  $\{(\pi d_v^2/4)\Delta p\}$  and the resultant of surface tension acting on the circumference at the cutting plane,  $\pi d_v \gamma_L$ , as shown in **Figure 1**[12].

$$d_v = \frac{4\gamma_L}{\Delta p} \quad (1)$$

where;

$\Delta p$ : internal pressure differential of internal void (Pa)

$\gamma_L$ : surface tension of paste (N/mm)

$d_v$ : diameter of internal void (mm)

On the other hand, the diameter of a surface void ( $d_{sv}$ ) is calculated using **Expression (2)**, which is a transformation of the balance between the resultant of internal pressure differential and surface tension. That is, a surface void adheres to the form as a result of its surface tension with contact angle ( $\theta_c$ ). In other word, the lower the value of  $\gamma_L$ , the smaller  $d_{sv}$  becomes.

$$d_{sv} = \frac{4\gamma_L}{\Delta p} \sin \theta_c \quad (2)$$

**Table 1** gives values of  $d_{sv}$  calculated using **Expression (2)** using the following data substitutions:  $\theta_c=90$  degrees,  $\gamma_L=73$ , 55, and 35 N/mm (values approximately equal to the surface tension of distilled water, the polycarboxylic acid SP, and the air-entraining agent, respectively). This table also shows that  $\gamma_L$  decreases when the SP and air-entraining agent (AE agent) are used. Eventually,  $d_{sv}$  also becomes smaller. Moreover, the decreasing length of the larger surface diameter of void which influence on appearance is longer than the smaller surface void.

(3) General conditions governing the movement of coarse aggregate and internal voids in self-compacting concrete

The settling of coarse aggregate particles in self-compacting concrete is explained in terms of the rheological constants: yield value( $\tau_y$ ) and plastic viscosity ( $\eta_p$ ). Certain assumptions are also made: coarse aggregate particles are

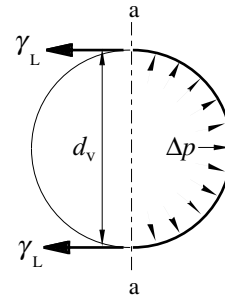


Fig.1 The internal forces acting on an internal void

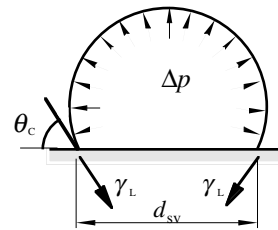
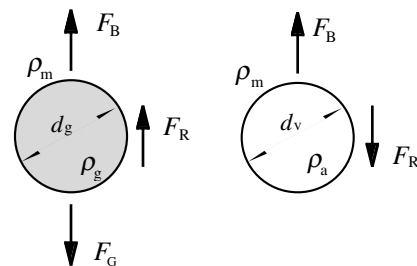


Fig.2 The internal forces acting on a surface void

Table1 The relationship between the diameter, internal pressure difference, and surface tension of surface void

$\Delta p$ (Pa)	$\gamma_L$ (N/mm)		
	73	55	35
5	$d_{sv}=60\text{mm}$	$d_{sv}=44\text{mm}$	$d_{sv}=28\text{mm}$
10	30	22	14
50	6	4.4	2.8
100	3	2.2	1.4
500	0.6	0.4	0.3
1000	0.3	0.2	0.1
2000	0.15	0.11	0.07
4000	0.08	0.06	0.04



coarse aggregate      internal void

Fig.3 The forces acting on coarse aggregate particles and internal void

assumed to be spherical solid bodies, the mortar in self-compacting concrete is taken to be a Bingham fluid, and bleeding is assumed to not occur. The forces acting on coarse aggregate particles are shown in the left-hand chart in **Figure 3**.

The forces acting on coarse aggregate particles are gravity ( $F_G$ ), buoyancy ( $F_B$ ), and fluid resistance ( $F_R$ ). These forces are calculated by using **Expressions (3)-(6)**.

$$F_G = \frac{\pi \cdot d_g^3}{6} \rho_g g \quad (3)$$

$$F_B = \frac{\pi \cdot d_g^3}{6} \rho_m g \quad (4)$$

$$F_R = 3\pi d_g^2 \left( \frac{v_g \cdot \eta_p}{d_g} + \alpha \tau_y \right) \quad (5)$$

$$F_R = 3\pi d_g^2 \left( \frac{v_g \cdot \eta_p}{d_g} + \frac{7\pi \cdot \tau_y}{24} \right) \quad (6)$$

where;  $F_G$ : gravity (N),  $F_B$ : buoyancy (N),  $F_R$ : fluid resistance (N),  $d_g$ : diameter of coarse aggregate (mm),  $\rho_m$ : density of mortar ( $\text{g/mm}^3$ ),  $\rho_g$ : density of coarse aggregate ( $\text{g/mm}^3$ ),  $v_g$ : settling velocity of coarse aggregate (mm/s),  $\eta_p$ : plastic viscosity of mortar (Pas),  $\tau_y$ : yield value of mortar (Pa)

**Expression (5)** is Ansley's expression, and it explains the fluid resistance when a sphere of diameter  $d_g$  moves in an incompressible Bingham fluid at velocity  $v_g$ . The numerical value of **Expression (5)** is a function of the Bingham number  $\{N_b = (d_g/v_g) (\tau_y/\eta_p)\}$ , and the average value of an ideal Bingham fluid is  $\alpha=7\pi/24$ . **Expression (6)** is obtained by substituting this value into **Expression (5)**. This relationship forms the principle of measurement of a ball-pulling viscometer, and can be used to accurately calculate the rheological constants of low-consistency paste, mortar, and concrete[13].

On the other hand, the rising of internal voids can be explained using the same assumptions as adopted for the coarse aggregate, simply substituting the coarse aggregate diameter ( $d_g$ ) in **Expressions (3), (4), and (6)** with the diameter of the internal voids ( $d$ ). Since  $F_G$  can be neglected because the density of air ( $\rho_a$ ) is extremely small compared to  $\rho_m$ , the forces acting on internal voids are  $F_B$  and  $F_R$ , as shown in the right-hand chart in **Figure 3**.

(4) Relationship between yield value of mortar and movement of coarse aggregate and internal voids

For coarse aggregate that remains stationary in the concrete, the settling velocity is 0 mm/s in **Expression (6)**. Then  $F_R$  is given by **Expression (7)** because it is only influenced by the yield value. Consequently, the coarse aggregate and mortar separate when  $F_G > F_B + F_R$ .

$$F_R = \frac{7\pi^2 d_g^2 \tau_y}{8} \quad (7)$$

There is a strong correlation between the mortar yield value and slump flow in self-compacting concrete, and the range of slump flow is 550-700 mm since, the yield value of mortar is restricted within limits.

The mortar yield value ( $\tau_y$ ) is estimated from the yield value of concrete ( $\tau_{yc}$ ), which is calculated from the slump flow. Here,  $\tau_{yc}$  is determined using **Expression (8)** referring to research by Kokado and others[14].

$$\tau_{yc} = \frac{15^2 \rho_c g V^2}{4\pi^2 S_f^5} \quad (8)$$

Where;  $\tau_{yc}$ : yield value of concrete (Pa),  $\rho_c$ : concrete density ( $\text{g}/\text{mm}^3$ ),  $g$ : gravitational acceleration ( $\text{mm}/\text{s}^2$ )  
 $V$ : capacity of slump cone ( $\text{mm}^3$ ),  $S_f$ : slump flow (mm)

This gives yield values of concrete of  $\tau_{yc}=70.0, 35.0,$  and  $20.0$  Pa corresponding to  $S_f=550, 630, 700$  mm; the ratio of these yield values is 2:1:0.57, based on  $S_f=630$  mm. Next, the yield value of mortar with  $S_f=630$  mm is assumed to be  $\tau_y=5.0$  Pa, and the yield value of other mortars is calculated using the same ratio of  $\tau_{yc}$ , resulting in  $\tau_y=10.0$  Pa,  $5.0$  Pa, and  $2.9$  Pa. These estimated values of  $\tau_y$  are lower than the usual value of  $\tau_y=2.2-22.0$  Pa[15]. Since these are apparent yield values measured with a rotational viscometer or similar, the true yield value needed to explain the migration of coarse aggregate and internal voids is smaller than the apparent value[16].

**Figure 4** shows the relationship between coarse aggregate, internal voids, and the forces acting on each particle with respect to  $\tau_y$ , with substitutions made for  $\rho_m=2.3 \times 10^{-3} \text{ g}/\text{mm}^3$  and  $\rho_g=2.67 \times 10^{-3} \text{ g}/\text{mm}^3$ .

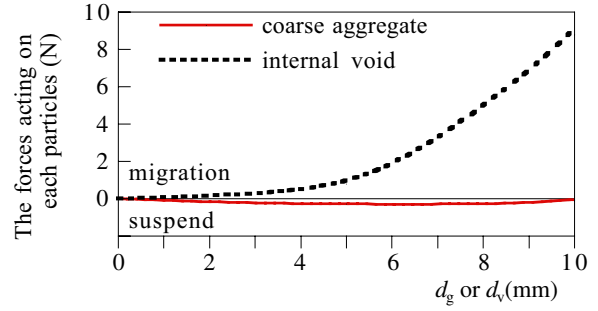
For  $\tau_y=2.9$ Pa in **Figure 4**, the coarse aggregate does not settle because acting force is  $F_G-(F_B+F_R)=0$  when  $d_g < 10$ mm. On the other hand, the coarse aggregate sinks when  $d_g > 10$ mm because  $F_G-(F_B+F_R) > 0$ . Moreover, coarse aggregate remains suspended in the mortar when  $\tau_y=5.0$  Pa and  $\tau_y=10.0$  Pa, and material segregation is not observed. These calculated results clearly reflect the overall characteristics of self-compacting concrete: coarse aggregate and mortar segregate when the slump flow is particularly high.

Internal voids rise regardless of  $\tau_y$  when  $d_v > 7$  mm. However, when  $d_v < 7$  mm, rising depends on  $\tau_y$ . **Figure 5** shows the minimum value of  $d_v$  at which rising results from  $F_B$ ;  $\tau_y$  is proportional to  $d_v$ . As noted above, the apparent yield value is  $\tau_{yc}=20.0-70.0$  Pa in concrete, and  $\tau_y=2.2-22.0$  Pa in mortar. Actually, the maximum diameter of internal voids in self-compacting concrete is around  $d_v=10.0$  mm. In other words, if the yield value of mortar is  $\tau_y=2.9-10.0$  Pa, the maximum diameter of internal voids can be estimated. As already noted, the migration of coarse aggregate and internal voids can be explained if the yield value of mortar is assumed to be  $\tau_y=2.9-10.0$  Pa.

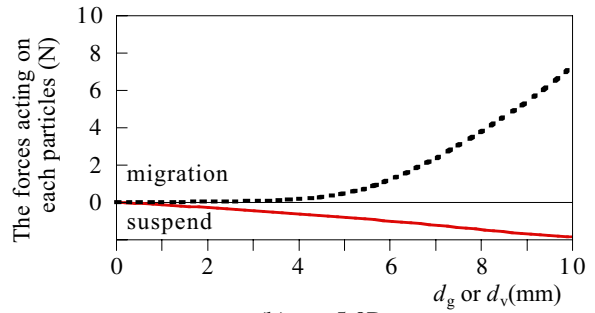
##### (5) Relationship between plastic viscosity of mortar and migration rate of internal voids

Internal voids rise in mortar when  $F_B > F_R$ , and the rise speed  $v_v$  is given by **Expression (9)** which is derived from the equilibrium between **Expressions (4)** and **(6)**.

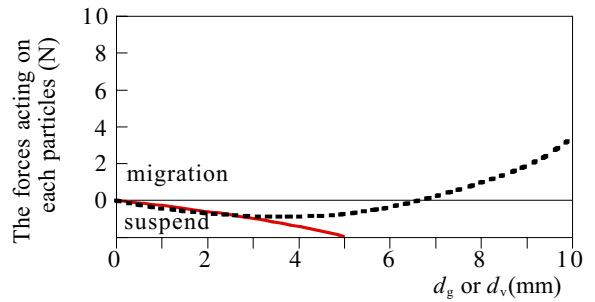
$$v_v = \frac{4d_v^2 \rho_m g - 21\pi d_v \tau_y}{72\eta_p} \quad (9)$$



(a)  $\tau_y=2.9$ Pa



(b)  $\tau_y=5.0$ Pa



(c)  $\tau_y=10.0$ Pa

**Fig. 4** The relationship between coarse aggregate, internal void, and the forces acting on each particles with respect to  $\tau_y$

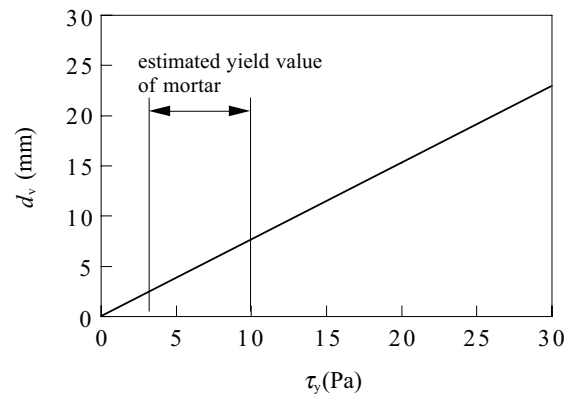


**Fig. 5** The minimum value of  $d_v$  at which rising results from  $F_B$

**Figure 6** shows the relationship between  $\eta_p$  and  $\nu_v$  for each  $\tau_y$ . It is clear from this figure that  $\nu_v$  is greatly influenced by variations  $\eta_p$ , the plastic viscosity of mortar ( $\eta_p=1.5-12.0$  Pas)[15]. Moreover,  $\nu_v$  fluctuates greatly when  $\tau_y$  and  $d_v$  vary, even if  $\eta_p$  remains constant.

In general, voids rise with a motion that avoids the coarse aggregate, which typically accounts for 30-35% of the volume of self-compacting concrete. Consequently, the apparent rise speed is less than this calculated value indicated in **Figure 6**. In other words, the quantity of voids in self-compacting concrete is influenced not only by the viscosity of the mortar but also by the bulk and shape of the coarse aggregate. Rise speed of the upper surface of the concrete ( $\nu_c$ ) must be less than  $\nu_v$  so as to discharge voids effectively. **Figure 6** also shows that an internal void with  $d_v > 10$  mm is discharged regardless of  $\tau_y$  in a normal self-compacting concrete placed at a rate of  $\nu_c = 5.0$  mm/s in the factory[17]. Moreover, with  $\tau_y = 2.9$  Pa or less, internal voids with  $d_v > 5$  mm are discharged regardless of  $d_v$ . On the other hand, internal voids with  $d_v < 5$  mm may be 1) discharged immediately after placing or 2) remain in the mortar, rising thereafter according to **Expression (9)**.

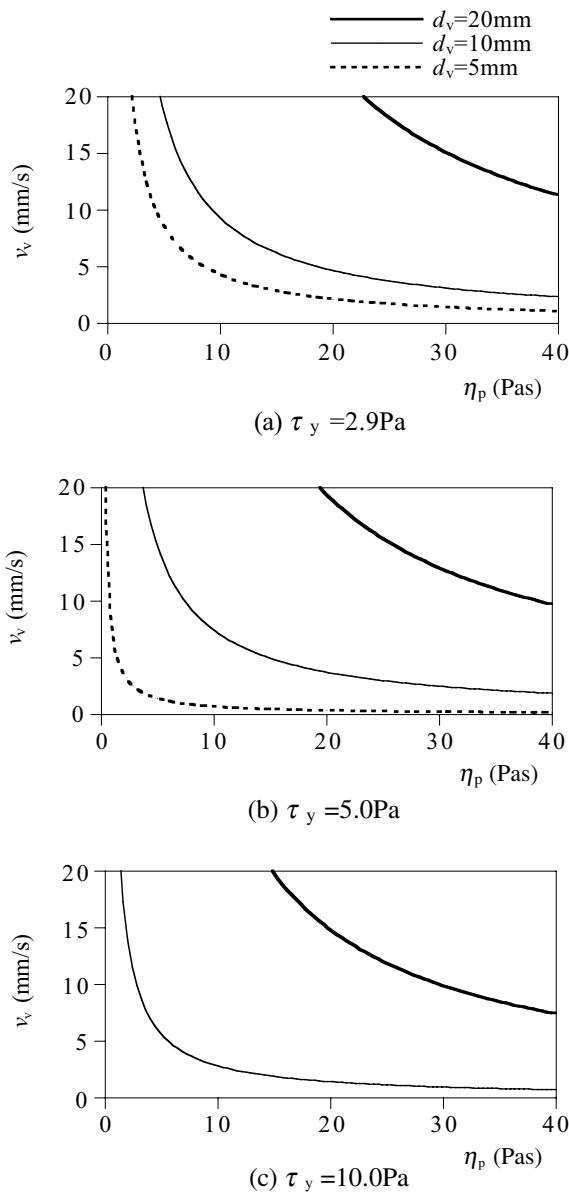


Fig.6 The relationship between  $\nu_v$  and  $\eta_p$  for each  $\tau_y$

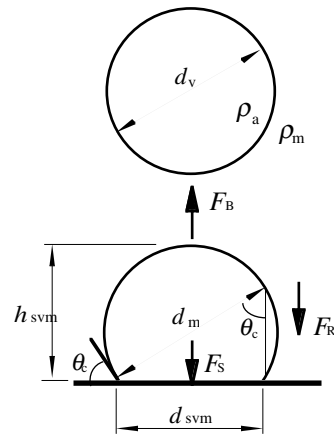


Fig.7 The outer forces acting on the surface void, and the adhered void

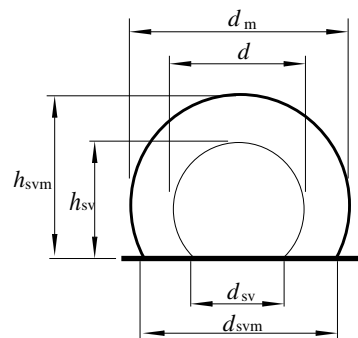


Fig.8 The dimensions of a surface void

(6) Condition for surface voids separating from form

Surface voids adhere to the form as a result of the surface tension of the cement paste, so adhesion ( $F_s$ ) depends on contact angle ( $\theta_c$ ) in addition to  $F_B$  and  $F_R$ , as shown in **Figure 7**. The dimensions of a surface void are defined in **Figure 8**. A surface void separates from the form when the void volume is such that  $F_B > F_R + F_S$  is satisfied. Moreover, surface void volume depends on  $\tau_y$  and  $\theta_c$ . The diameter of the opening (the diameter of the void at the surface) also has an upper limit for each  $\tau_y$  and  $\theta_c$ . The maximum diameter of a void at the surface is expressed as  $d_{svm}$ , and is calculated under the following conditions: 1) the volume of a separated void ( $V_v$ ) immediately after separation is equal to the volume of the surface void ( $V_{svm}$ ), or  $V_v = V_{svm}$ ; and 2) the equilibrium of forces applies to the surface void ( $F_B = F_R + F_S$ ).

**Expressions (10)-(16)** are used to calculate  $d_{svm}$ .

$$V_v = \frac{\pi \cdot d_v^3}{6} \quad (10)$$

$$V_{svm} = \pi \left( \frac{d_{svm} h_{svm}^2}{2} - \frac{h_{svm}^3}{3} \right) \quad (11)$$

$$\frac{d_v \sin^3 \theta_c}{2} - \frac{d_{svm}^3 (1 + \cos \theta_c)^2 (2 - \cos \theta_c)}{8} = 0 \quad (12)$$

$$F_B = \frac{\pi \cdot d_v^3}{6} \rho_m g \quad (13)$$

$$F_R = \frac{7\pi^2}{2} \left( \frac{d_m}{2 \sin \theta_c} \right)^2 \tau_y \quad (14)$$

$$F_S = \pi \cdot d_{svm} \sin \theta_c \gamma_L \quad (15)$$

$$\frac{\pi \cdot d_v^3}{6} \rho_m g - \frac{7\pi^2 \tau_y}{2} \left( \frac{d_m}{2 \sin \theta_c} \right)^2 - \pi \cdot d_{svm} \sin \theta_c \gamma_L = 0 \quad (16)$$

First,  $V_v$  is calculated using **Expression (10)** and  $V_{svm}$  is obtained with **Expression (11)**. At the point when a surface void separates from the form, the relationship between  $d_{svm}$ ,  $d_m$ , and  $\theta_c$  at  $V_v = V_{svm}$  is given by **Expression (12)**, because  $d_{svm} = d_m \sin \theta_c$ , and  $h_{svm} = d_m (1 + \cos \theta_c) / 2$ . Finally,  $F_B$ ,  $F_S$ , and  $F_R$  calculated using **Expressions (13)**, **(14)**, and **(15)** are transformed into **Expression (16)** because of the equilibrium of these three forces.

The relationship between  $d_{svm}$  and  $\tau_y$  for each  $\theta_c$  is calculated using **Expressions (12)** and **(16)**, as shown in **Figure 9**, in which substitutions are made for  $\rho_m = 2.3 \times 10^{-3} \text{ g/mm}^3$ ,  $g = 9,800 \text{ mm/s}^2$ , and  $\gamma_L = 73 \text{ N/mm}$ . As  $d_{svm}$  increases, so  $\tau_y$  also becomes larger, and this tendency is clear when  $\theta_c$  is large, as shown in the figure. Moreover, the diameter of surface voids is  $d_{svm} > 0$  at  $\tau_y = 0.0 \text{ Pa}$ , corresponding to a Newtonian fluid. In other words, there is a limit to the size of surface voids that adheres to the form at  $\tau_y = 0.0 \text{ Pa}$ .

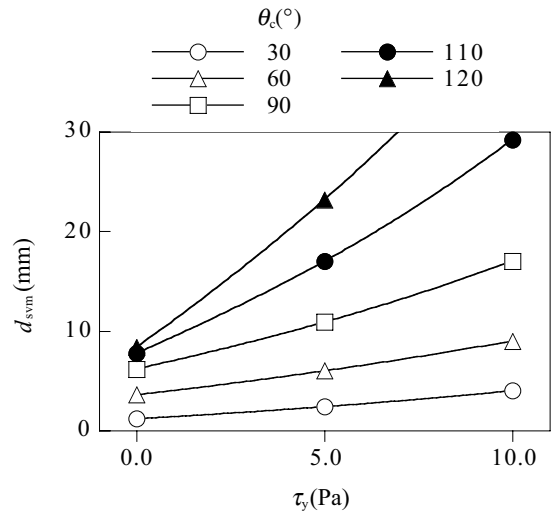


Fig.9 The relationship between  $d_{svm}$  and  $\tau_y$  for each  $\theta_c$

Table2 Materials used

Materials	Type and physical properties	
Cement	I , II	ordinary portland cement, $\rho_c=3.15 \text{ g/cm}^3$
Blast-furnace slag	I , II	blaine specific area=6000cm <sup>2</sup> /g, $\rho_b=2.91 \text{ g/cm}^3$
Fine aggregate	I	sea sand, $\rho_s=2.58 \text{ g/cm}^3$ , FM=2.80
	II	sea sand, $\rho_s=2.51 \text{ g/cm}^3$ , FM=2.90
Coarse aggregate	I	crushed stone, Maximum size=20mm, $\rho_g=2.73 \text{ g/cm}^3$ FM=6.77
	II	crushed stone, Maximum size=20mm, $\rho_g=2.67 \text{ g/cm}^3$ FM=7.01
Superplasticizer	I	naphthalene-based type
	II	polycarboxylic acid type
Air adjusting agent	I	air-entraining agent
	II	defoaming agent

I is a case of naphthalene-based SP, II is a case of polycarboxylic acid SP

Table3 Mix proportion for concrete with an air content of 1.5%

Max. size (mm)	Slump-flow (cm)	Air (%)	W/(C+BS) (%)	s/a (%)	Unit weight(kg/m <sup>3</sup> )					
					W	C	BS	S	G	SP
20	63 ± 3	1.5 ± 0.5	31.6	51.6	178	236	327	826	819	5.9
								804	816	

In the column of S and G in the table, the upper and lower part are the cases of naphthalene-based SP and polycarboxylic acid SP respectively.

The surface void contact angle in specimens fabricated by the authors was  $\theta_c < 90$ . Moreover, when  $\tau_y = 10.0 \text{ Pa}$ , reflecting the minimum slump flow of  $S_f = 550 \text{ mm}$  at which filling is possible without compaction, the maximum surface void diameter is  $d_{svm} = 17.0 \text{ mm}$  in **Figure 9**. This is the actual maximum value of surface void diameters. The maximum diameter can be explained in this way because of the equilibrium of the forces acting on surface voids by which the yield value of mortar is considered.

### 3. OUTLINE OF EXPERIMENT

#### (1) Density and surface tension of chemical admixture

According to prior research by the authors, the surface tension of the paste does not change with time after mixing[18]. However, the relationship between the surface tension of chemical admixtures and the surface tension of the paste has not been previously clarified. To clarify this relationship, three types of chemical admixture, naphthalene-based SP, polycarboxylic acid SP, and an AE agent, were diluted with distilled water for measurement of the relationship between density of chemical admixture and surface tension. Surface tension measurements were made using a dü-Nouy type of surface tension meter.

#### (2) Type of SP, air adjusting method, and properties of surface voids

##### a) Materials used and concrete mix proportion

The self-compacting concrete contained powder of which 60% by volume was blast-furnace slag. The target values for slump flow and air content were 630 mm and 5.0%, respectively. An air content of 9% was achieved by using a polycarboxylic acid SP and by adding 1.5%, 5.0%, and 9.0% of the naphthalene-based SP. The materials used are shown in **Table 2**. The mix proportion for concrete with an air content of 1.5% is shown **Table 3**. An AE agent was used with the naphthalene-based SP to adjust the air content, and an defoaming

agent was used with the polycarboxylic acid SP.

#### b) Manufacture of specimens

A double-axial mixer of 55 liters capacity was used to mix the concrete. Batches of 35 liters were mixed at one time. The materials were added to the mixer in the order aggregate and powder, then water and SP, and the mixing times were 30 seconds and 120 seconds. Steel forms were used. Specimens measured 500 mm high, 80 mm thick, and 300 mm wide. A commercially available non-stick oily-type form-releasing agent (with a principal component consisting of a paraffin-type hydrocarbon) was lightly sprayed over the form with an atomizer and wiped with absorbent cotton for an hour before placing the concrete mixture. Concrete was dropped freely from the top of the form, and placing took place continuously for 90 seconds starting at the center.

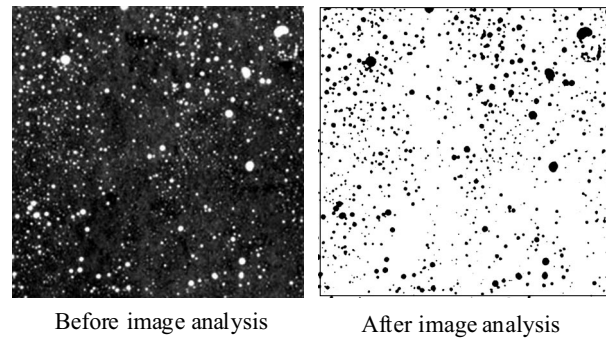


Fig.10 The pictures of surface void

#### c) Quantification of surface voids

The area and distribution of surface voids were examined on the vertical surface measuring 300 mm in width and 500 mm in height by image analysis. First, the concrete surface was washed with acetone and then spread with black oily ink. Surface voids were filled with blast-furnace slag powder, making them stand out for image analysis. Pictures were taken of the concrete surface with a digital camera, and the results loaded into a personal computer(**Figure 10**).

The measures used to represent surface voids are the surface void area ratio ( $A_{sv}$ ):the ratio of the area of surface void to concrete surface area, the maximum diameter of surface void ( $d_{max}$ ), and the number of surface voids ( $N_{sv}$ ), having void diameter larger than of 1 mm was considered as circle.

#### (3) Rheological constants of mortar and characteristic of surface void assumed from slump flow of concrete

##### a) Materials used and mix proportion of concrete

The materials used are shown in **Table 2** and the concrete mix proportion is shown in **Table 3**.

##### b) Fabrication of specimens

The mixing method, specimen size, materials, and form were as described in the previous section. Three types of form-releasing agent were used to adjust the contact angle ( $\theta_c$ ): two oily types and one watery type. Placing was carried out with rise speeds  $v_c=5.6, 2.7,$  and  $2.1$  mm/s so as to examine the influence of rise speed on surface voids.

##### c) Quantification of surface voids

The area and distribution of surface voids were examined by image analysis as described in the previous section. A mathematical model with  $\theta_c$  of the surface void was assumed to be a part of the sphere. The maximum depth of surface void ( $h_{sv}$ ) and circle conversion diameter ( $d_{sv}$ ) was measured using a laser displacement gage and image analysis, then  $\theta_c$  was calculated by the inclination of the recurrence straight line ( $h_{sv}/d_{sv}$ ).

## 4. RESULTS AND DISCUSSION

### (1) Density and surface tension of chemical admixture

**Figure 11** shows the relationship between density and surface tension of the chemical admixtures. In the case of the naphthalene-based SP, the surface tension is almost equal to that of distilled water,  $\gamma_L=73$  N/mm, and is

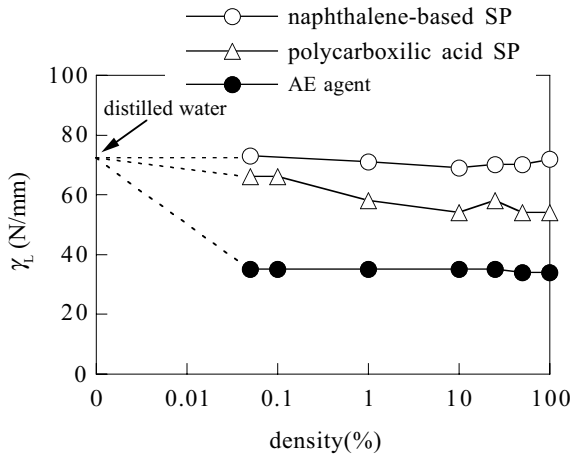


Fig.11 The relationship between density and surface tension of the chemical admixtures

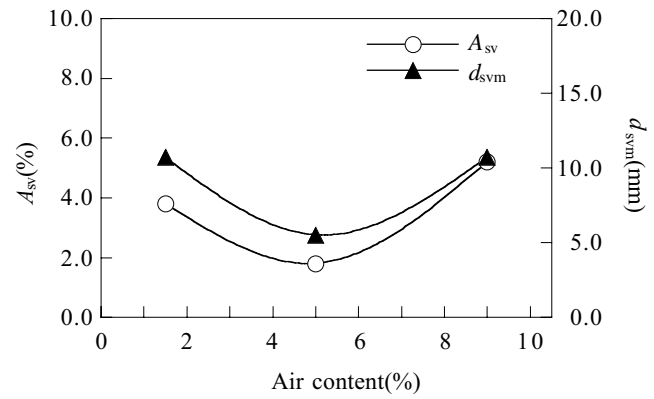


Fig.12 The relationship between surface void area ratio( $A_{sv}$ ) and maximum diameter of surface void( $d_{svm}$ ) for each air content [In case of naphthalene-based SP]

not influenced by density. On the other hand, with the polycarboxylic acid SP, at densities of 1% or less the surface tension decreases as density is increased. However, when the density is 1% or more, the surface tension remains constant.

In general, the SP content in powder-type self-compacting concrete is 0.5-3.0% of the mass[19]. If powder content is  $550 \text{ kg/m}^3$  and the water content  $175 \text{ kg/m}^3$ , the density of the SP is 1.6-9.4% of the water content. **Figure 11** shows the surface tension of a watery solution of SP in the density range of 1.6-9.4%. This is the same as the surface tension of the SP. This means that the surface tension of paste can be estimated as equal to the surface tension of the SP.

Moreover, the surface tension of the AE agent is  $\gamma_L=35 \text{ N/mm}$ , the smallest of the three types of chemical admixture studied in this experiment. The AE agent is used at ratios of about 10% of the SP content, and even a small amount reduces the surface tension of the paste remarkably. Incidentally, the surface tension of a watery solution of SP with the AE agent has the same surface tension as the AE agent itself, though this is not shown in the figure.

## (2) Type of SP, method of adjusting air content, and properties of surface voids

### a) Use of naphthalene-based SP together with AE agent

**Figure 12** shows the relationship between surface void area ratio ( $A_{sv}$ ) and maximum diameter of surface void ( $d_{svm}$ ) for each air content.

Even though  $A_{sv}$  is 3.8% at an air content of 1.5%, it decreases to 1.8% when the air content is adjusted to 5.0% with the AE agent. That is, the surface voids become smaller because  $\gamma_L$  decreases. However,  $A_{sv}$  when increased to 5.2% the corresponding amount of AE agent is also increased to adjust the air content to 9.0%.

Moreover, when  $d_{svm}=10.7\text{mm}$ ,  $5.5\text{mm}$ , and  $10.7\text{mm}$  to the air contents of 1.5%, 5.0%, and 9.0% respectively, was minimized at the air content is 5.0% as well as  $A_{sv}$ . Thus,  $d_{svm}$  was reduced by half to 5.5 mm in the case of concrete with an air content of 5.0% while the  $d_{svm}$  value of plain concrete was 10.7 mm. This reflects a decrease in surface tension of the paste from  $\gamma_L=73 \text{ N/mm}$  to  $\gamma_L=35 \text{ N/mm}$ . The size of actual surface voids can be inferred from **Expression (2)** introduced earlier.

The higher  $d_{svm}$  at an air content of 9.0% is thought to be attributable to a number of factors: 1) the migration of large voids is hampered by the many fine internal voids; 2) when voids are close together, they begin to combine; 3) the buoyancy acting on the voids decreases as the density of the mortar decreases.

The distribution of the number of surface voids ( $N_{sv}$ ) of each diameter  $d_{sv}=1.0 \text{ mm}$  is shown in **Figure 13**. In

this figure,  $d_{sv}$  is clear and no difference depending on air content is seen when  $N_{sv}$  is 3.0 mm or more. On the other hand,  $d_{sv}$  increases with  $N_{sv}$  when  $d_{sv}$  is 3.0 mm or less. In particular, the rise in  $N_{sv}$  when  $d_{sv}=1.0-1.9$  mm is quite large when the air content is 9.0%. Thus,  $d_{sv}$  changes even if the air content is enhanced using the AE agent and the number of surface voids 2.0 mm or more in diameter does not change.

As already noted, when the AE agent was added to the naphthalene-based SP and the air content was also adjusted to around 5.0%, the generation of surface voids was suppressed. The many minute surface voids of  $d_{sv}=1.0$  mm or less generated large air content, it is necessary to examine a suitable method of suppressing the appearance of minute surface voids.

b) Use of polycarboxylic acid SP together with defoaming agent

**Figure 14** shows  $A_{sv}$  and  $d_{svm}$  with respect to air content for two levels of air content: 1.5% and 5.0%. In the figure,  $A_{sv}$  and  $d_{svm}$  are almost equal regardless of air content, in contrast with the results for the naphthalene-based SP.

The  $N_{sv}$  for each  $d_{sv}=1.0$  mm is shown in **Figure 15**. In the case of an air content of 1.5% and added defoaming agent,  $N_{sv}$  for  $d_{sv}=1.0-1.9$  mm is lower. However, the air adjustment is suppressed and even if the defoaming agent is added to the polycarboxylic acid SP, the generation of a big surface void cannot be suppressed as aimed because the amount of generation of the surface void of  $d_{sv}=2.0$ mm or more which spoils the appearance does not change at all.

As mentioned above, AE agent and defoaming agent were used together with the naphthalene-based SP and the polycarboxylic acid SP, respectively, to adjust the air content. The relationship between air content and surface void generation was examined. The generation of surface voids was found to be independent of air content, but the number of surface voids decreased as the surface tension of the paste fell.

(3) Rheological constants of mortar assumed from slump flow and properties of the surface voids

a) Yield value of mortar and the properties of surface void

The relationships between surface void area ratio ( $A_{sv}$ ), maximum diameter of surface voids ( $d_{svm}$ ), and yield value of the mortar ( $\tau$ ) are shown in **Fig-**

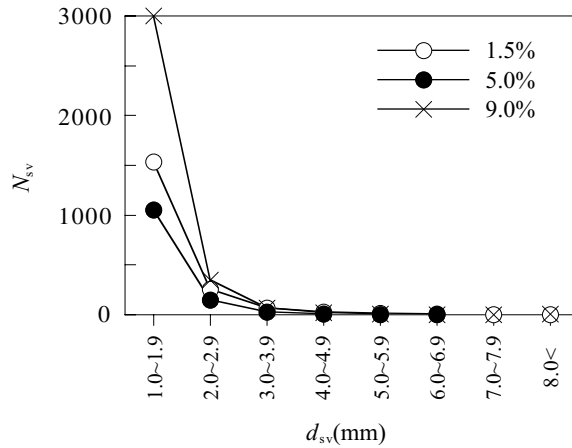


Fig.13 Number of surface void( $N_{sv}$ ) for each  $d_{sv}=1.0$ mm [In case of naphthalene-based SP]

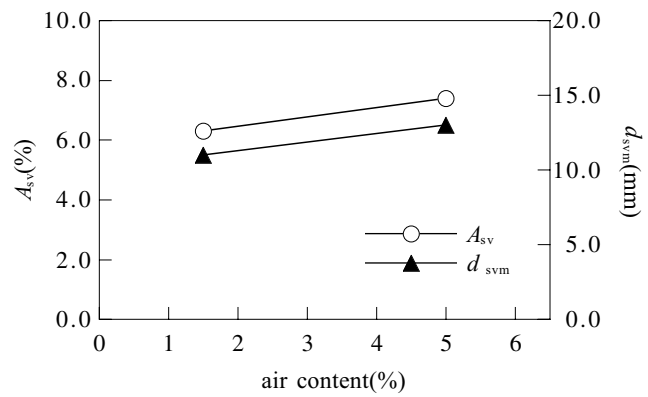


Fig.14 The relationship between surface void area ratio( $A_{sv}$ ) and maximum diameter of surface void( $d_{svm}$ ) for each air content [In case of polycarboxylic acid SP]

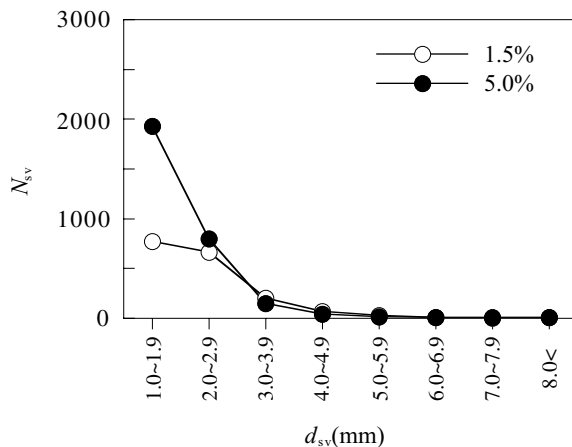


Fig.15 The distribution of the number of surface void( $N_{sv}$ ) for each  $d_{sv}=1.0$ mm [In case of polycarboxylic acid SP]

**Figure 16.** The horizontal axis represents  $\tau_y$  which is assumed from slump flow of the concrete:  $\tau_y=2.9, 5.0, \text{ and } 10.0 \text{ Pa}$  is equivalent to  $S_f=700, 630, \text{ and } 550 \text{ mm}$ , respectively. And, when  $\tau_y$  is small,  $A_{sv}$  and  $d_{svm}$  are also small, so the generation of surface voids is difficult.

The range of slump flows in ordinary powder-type self-compacting concretes is  $S_f=500\text{-}700 \text{ mm}$ . Because 70% or more of slump flow of supply is  $S_f=600\text{-}700\text{mm}$  in general self-compacting concrete, which is classified into mixing which the surface void is not easily generated[16]. If a better appearance is required, the only requirement is for  $S_f$  to be 700 mm or more.

**Figure 17** shows the relationship between theoretical and experimental values of  $d_{svm}$ . In the evaluation of  $\theta_c$ , the shape of the surface void is assumed to be a partial sphere, and the inclination of the approximate straight line ( $h_{sv}/d_{sv}$ ) is  $h_{sv}/d_{sv}=0.44$ . To allow easy calculation of the following,  $\theta_c$  is assumed to be 90 degrees, though in the experiment its value was  $\theta_c=97$  degrees, as calculated from  $h_{sv}/d_{sv}=0.44$ .

In the same figure, the theoretical and experimental values of  $d_{svm}$  correspond well. This means that  $d_{svm}$  can be determined from the equilibrium of the three forces acting on the surface void: buoyancy ( $F_b$ ), adhesion ( $F_s$ ), and fluid resistance ( $F_r$ ) (considered as  $\tau_y$ ). In **Figure 17**, incidentally, the difference between the theoretical and experimental values increases when  $\tau_y=2.9 \text{ Pa}$  or less, and when  $\tau_y=10.0 \text{ Pa}$  or more. However, the range of  $\tau_y$  in self-compacting concrete is  $\tau_y=2.9\text{-}10.0 \text{ Pa}$ , as already mentioned, so this is not an issue.

In **Figure 16**,  $A_{sv}$  and  $d_{svm}$  are estimated to be  $A_{sv}=1.5\%$  and  $d_{svm}=5.1 \text{ mm}$  at  $\tau_y=0.0 \text{ Pa}$  by exponential approximation. Surface voids remain evenly distributed when  $\tau_y=0.0 \text{ Pa}$  of the yield value of the Newtonian fluid from the above-mentioned one. Because the theoretical  $d_{svm}$  (6.2 mm) at  $\tau_y=0.0 \text{ Pa}$  and the experimental value (5.1 mm) are close, it can be inferred that the assumptions made in the calculation are valid.

**Figure 18** shows experimental values of  $A_{sv}$  and  $d_{svm}$  for each  $\theta_c$ , which depends on the type of form-release agent: one watery type and two oily types. Along the horizontal axis,  $\theta_c=60$  degrees represents the watery form-release agent, while  $\theta_c=90$  degrees and 110 degrees represent the oily form-release agents, as calculated from  $h_{sv}/d_{sv}$ . At smaller values of  $\theta_c$ ,  $A_{sv}$  and  $d_{svm}$  also become small, and appearance improves. Lower values of  $\theta_c$  are associated with reduced surface void area because surface voids remain inside the concrete. When a watery form-release agent is used, almost all surface voids remain invisible because they are covered with a thin layer of cement paste. This figure represents only measured surface voids; invisible voids are not included.

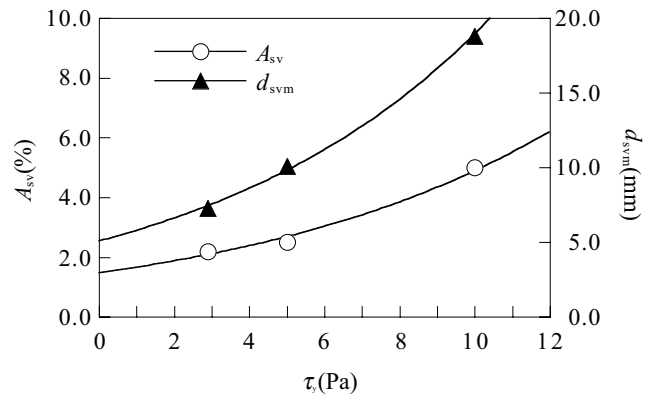


**Fig.16** The relationship between surface void area ratio( $A_{sv}$ ), maximum diameter of surface void( $d_{svm}$ ), and yield value of mortar( $\tau_y$ )

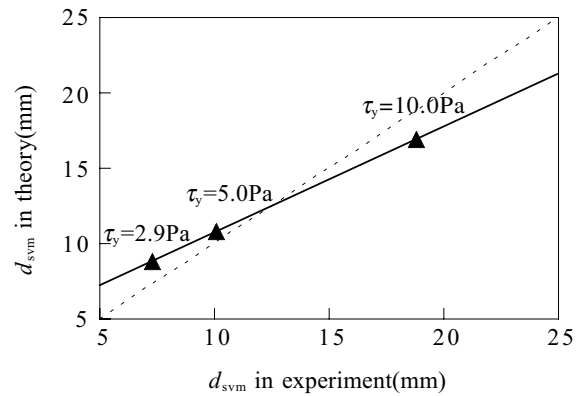


**Fig.17** The relationship between the theoretical and experimental values of  $d_{svm}$

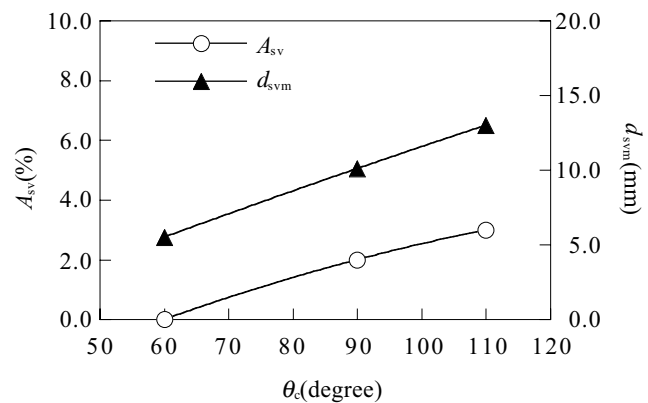


**Fig.18** Experimental values of  $A_{sv}$  and  $d_{svm}$  for each  $\theta_c$

**Figure 19** compares theoretical and experimental values of  $d_{svm}$  for each value of  $\theta_c$ . This figure also indicates that, even with varying  $\theta_c$ , the size of surface voids can be explained by the equilibrium of forces acting on them.

The relationship between  $d_{svm}$  and  $\theta_c$  for each  $\tau_y$  is shown in **Figure 20**, which expresses the theoretical values of **Figure 9** and the experimental values of **Figure 18**. This figure also demonstrates that, when  $\tau_y$  is small,  $d_{svm}$  becomes small as long as  $\theta_c=60$  degrees or more, but as  $\tau_y$  becomes larger,  $d_{svm}$  also becomes increasingly large.

b) Plastic viscosity of mortar and properties of surface voids

Surface voids separate from the form in two different ways, as follows. First, in the case of a horizontal form, surface voids part from the form and immediately become internal voids. Second, in the case of a vertical form, surface voids rise along the form until they are eventually discharged from the surface of the concrete at the placing plane. For all forms except horizontal or near-horizontal ones, plastic viscosity ( $\eta_p$ ) influences the separation of surface voids. For instance, a surface void on a vertical form rises along the form when  $F_b > F_R + \beta F_s$  (where  $\beta$  is a coefficient representing the influence of the form inclination angle). The rise speed of a surface void ( $v_{sv}$ ) in this situation is calculated using **Expression (9)**. When  $\eta_p$  is small,  $v_{sv}$  becomes large, and the surface void is easily discharged at the surface. In fact, a large surface void that would have an impact on the appearance of the finished concrete will be discharged if the raise rate during concrete placing ( $v_c$ ) is smaller than  $v_{sv}$ , so  $\eta_p$  has little influence. **Figure 21** shows experimental values of  $A_{sv}$  and  $d_{svm}$  with respect to  $v_c$ . It is clear that  $A_{sv}$  is high when  $v_c$  is large. On the other hand,  $d_{svm}$  falls with  $v_c$  for  $v_c < 2.8$  mm/s, and is almost constant for  $v_c > 2.8$  mm/s. Thus, if  $v_c$  is small, the influence of  $\eta_p$  on the generation of surface voids is smaller than that of  $\tau_y$  and  $\theta_c$ .

Further, if the form is subjected to low-frequency vibration (20-30 Hz),  $\eta_p$  influences the migration of surface voids. Fluid resistance ( $F_R$ ) decreases as  $\tau_y$  decreases when the concrete is subject to vibration. As a result, the migration of surface voids is activated. In this case, the surface void rise mechanism can be explained using **Expression (9)**, and the minimum required vibration time can be calculated using  $v_{sv}$  and the distance to the discharge plane. This enables the separation of coarse aggregate and mortar to be minimized while reducing the concentration of internal voids on the mould and shortening construction time.

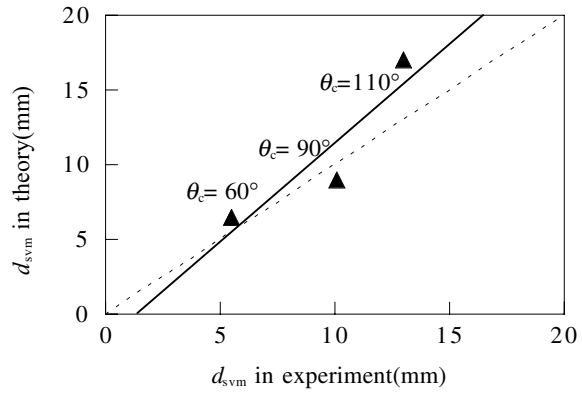


Fig.19 Compares of thoretical and experimental values of  $d_{svm}$  for each  $\theta_c$

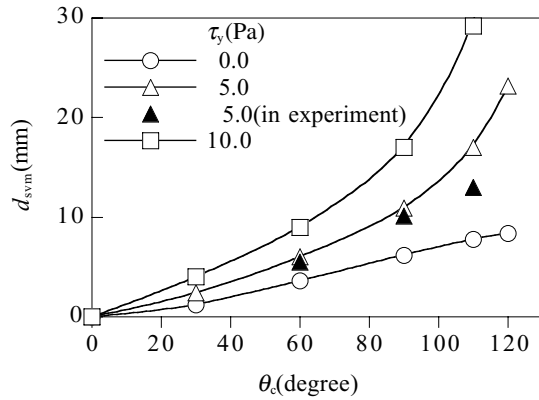


Fig.20 The relationship between  $d_{svm}$  and  $\theta_c$  for each  $\tau_y$

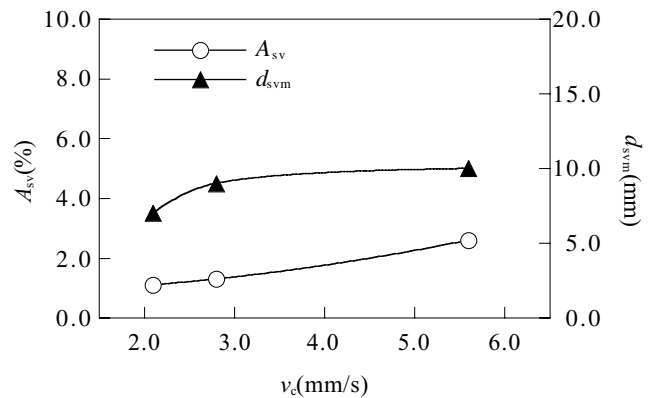


Fig.21 Experimental values of  $A_{sv}$  and  $d_{svm}$  with respect to  $v_c$

## 5. SUMMARY

This research has clarified the following points.

- (1) Adding an AE agent to a naphthalene-based superplasticizer such that the air content reaches around 5.0% reduces the surface tension of the paste. As a result, surface voids are reduced in size and the appearance of the concrete improves. On the other hand, the use of a defoaming agent in combination with a polycarboxylic acid superplasticizer to adjust the air content has no effect on the quantity of surface voids. Thus the generation of surface voids depends on the type and combination of chemical admixtures, and cannot be inferred from the air content alone.
- (2) If internal voids are treated as solid spherical bodies, their theoretical maximum diameter in self-compacting concrete ( $d_{vm}$ ) is found to be around 7.0 mm from the equilibrium of forces acting on them: buoyancy, gravity, and fluid resistance. Moreover, the same treatment can be applied to the segregation of coarse aggregate and mortar.
- (3) When the slump flow is  $S_f=550-700$  mm and the contact angle is  $\theta_c=30-90$  degrees, the maximum diameter of a surface void ( $d_{svm}$ ) can be calculated as  $d_{svm}=2.0-17.0$  mm from the equilibrium of forces acting on the void and adhesion to the form due to paste surface tension.
- (4) In case of oily form-release agents, the larger  $\theta_c$  and adhesion makes  $d_{svm}$  larger also. On the other hand, the  $\theta_c$  value when a watery form-release agent is used becomes  $\theta_c=0$  degrees, so almost all surface voids are hidden by a thin film of cement paste.
- (5) The plastic viscosity of mortar ( $\eta_p$ ) influences the rise speed of surface voids ( $v_{sv}$ ). When  $\eta_p$  is small,  $v_{sv}$  is higher. Moreover, if the placement raise speed is less than  $v_{sv}$ ,  $\eta_p$  does not influence the size of the surface voids.

## Reference

- [1] Keiichi, Y, "Introduction and Usage Prospects for Highly Flowable Concrete at Plants of Precast Concrete Product", Cement & Concrete, No.585, pp.9-14,1995( in Japanese )
- [2] Kawashima, M., et al., "Use of High Fluidity Concrete in the Production of Precast Concrete Products", CONCRETE JOURNAL, Vol.38, No.5, pp.51-54, 2000( in Japanese )
- [3] Ichimiya, K., et al., "Influences of Surface-Air-Bubbles on Durability of High Fluidity Concrete Products", The proceedings of the 53rd JSCE Annual Meeting, pp.408-409, 1998( in Japanese )
- [4] Yamato, F., et. al., "Study on Decreasing Method of Surface Voids on Concrete", Proceedings of the Japan Concrete Institute, Vol.8, pp.253-256, 1986( in Japanese )
- [5] Ichimiya, K., et al., "Influence of Placing Conditions on Air Void Characteristics at the Surface of High Fluidity Concrete", Proceedings of JCI, Vol.19, pp.61-66, 1997( in Japanese )
- [6] Zhixiang, L., et al., "A Study on Surface Air Voids of High Flowable Concrete Containing Powdered Material, Cement Science and Concrete Technology", No.52, pp.986-991, 1998( in Japanese )
- [7] Kazuhiro, Y., et al., "Study on Appearance of the Surface of Hardened Highly Workable Concrete", JCA PROCEEDINGS OF CEMENT & CONCRETE, No.49, pp.576-581, 1995( in Japanese )
- [8] Jiroh, M., et al., "Science and Technology for Concrete", Sankaido, pp.108-112, 1996( in Japanese )
- [9] Ichimiya, K., et al., "Behavior of Surface Voids in Self-Compacting Concrete with Low-Frequency Vibration", TRANSACTIONS OF THE JAPAN CONCRETE INSTITUTE, Vol.23, pp.413-418, 2002
- [10] JSCE, "Concrete Library Recommendation for Construction of Self-Compacting Concrete", pp.207-208, 1998( in Japanese )
- [11] Kyushu Branch of JCI, "Standard of Admixture and Performance of Concrete", pp.96,1999( in Japanese )
- [12] Kenichi H., "Bubbles of Washing and Voids in Concrete", Japan Cement Association, pp.75-81, 1985( in Japanese )
- [13] JSCE, "Proceedings of the Symposium on Properties of Fresh Concrete and their Application in Concreting Practice", pp.190-192, 1986( in Japanese )
- [14] Kokado, T., et al., "Study on a Method of Obtaining Rheological Coefficients of High-flow Concrete from Slump Flow Test", Journal of Materials, Concrete Structures and Pavements of JSCE, pp113-130, 1999( in Japanese )

- [15] Architectural Institute of Japan, "Recommendations for Mix Design and Construction Practice of High Fluidity Concrete", pp.135-144, 1997( in Japanese )
- [16] Powers, T.C., "The Properties of Fresh Concrete", pp.437-532, 1968
- [17] Nagao, K., et al., "Experimental examination concerning surface void of concrete products using self-compacting concrete", Proceedings of 51st JSCE Annual Meeting, pp.656-657, 1996( in Japanese )
- [18] Ichimiya, K., et al., "Influence of the Wettability and Angle of Form on the Characteristics of Surface Voids in Self-Compacting Concrete", Journal of Materials, Concrete Structures and Pavements, No.704/V-55, pp.143-150, 2002( in Japanese )
- [19] JSCE, "Concrete Library Recommendation for Construction of Self-Compacting Concrete", pp.181-182, 1998( in Japanese )